Earth and Space Science

METHOD
10.1029/2020EA001611

Key Points:

- A systematic method to generate approximate scalebars for obliquely acquired Martian landscape images was developed
- A newly created Approximate Scale for Images and Chemistry (ASIC) website links images, color, spatial scale, and chemistry, as returned by NASA's Curiosity rover in Gale crater
- The ASIC website is complementary and strongly linked to the Analyst's Notebook, the data resource for Martian/lunar landed missions

Supporting Information:

Supporting Information may be found in the online version of this article.

Correspondence to:

W. Goetz,
walter.goetz@mail.de

Citation:

Goetz, W., Bruns, M., Thoma, S., Pardowitz, I., & Stein, T. C. (2023). Determination of spatial scale in Martian landscape images acquired by the Curiosity rover, and viewing image scale and target chemistry using the ASIC website. *Earth and Space Science*, *10*, e2020EA001611. https://doi.org/10.1029/2020EA001611

Received 1 JAN 2021
Accepted 1 APR 2023

Author Contributions:

Conceptualization: Walter Goetz, Stephan Thoma, Iancu Pardowitz, Thomas C. Stein
Data curation: Michael Bruns, Thomas C. Stein
Methodology: Walter Goetz, Iancu Pardowitz, Thomas C. Stein
Project Administration: Walter Goetz
Resources: Thomas C. Stein

© 2023 The Authors. Earth and Space Science published by Wiley Periodicals LLC on behalf of American Geophysical Union.
This is an open access article under the terms of the Creative Commons Attribution License, which permits use, distribution and reproduction in any medium, provided the original work is properly cited.

Determination of Spatial Scale in Martian Landscape Images Acquired by the Curiosity Rover, and Viewing Image Scale and Target Chemistry Using the ASIC Website

Walter Goetz[1,2], Michael Bruns[1], Stephan Thoma[1], Iancu Pardowitz[1], and Thomas C. Stein[3]

[1]Max Planck Institute for Solar System Research (MPS), Göttingen, Germany, [2]Geoscience Center, Department of Geobiology, Georg-August-Universität Göttingen, Göttingen, Germany, [3]Washington University, St. Louis, MO, USA

Abstract In this paper we describe a method to compute spatial scales for images acquired by NASA's Mars Curiosity rover (Mars Science Laboratory, MSL). The method is based on the assumption that the rover stands on an infinite plane that may have any orientation with respect to the local gravity vector. While not new, it is the first time that this method is systematically applied to Martian images acquired by a lander. A continuously run software pipeline processes the images acquired by the rover within a 20 m radius, adds approximate scalebars to the raw images, and generates, whenever possible, rectified (warped) versions of those images. The products of this software pipeline and the chemical compositions of relevant rover science targets from NASA's Planetary Data System archive, are made available to the public via the Approximate Scale for Images and Chemistry website, which has been developed in collaboration with the Planetary Data System Analyst's Notebook for the MSL mission. Hyperlinks connect the two resources.

Plain Language Summary We developed a software pipeline that calculates the spatial scale of images acquired by NASA's Mars Curiosity rover. The software pipeline is linked to a new website: the Approximate Scale for Images and Chemistry, in which the scalebar products are paired with information about the shape, size, color, and chemical composition of the imaged site, obtained by the rover suite of instruments. The images mimic the vantage point of human eyes and are therefore well-suited to inspire field geologists (including those mainly working on Earth) to interpret Martian geologic features.

1. Introduction

Imaging of the Martian surface at different (overlapping) spatial scales, in particular at orbital (kilometer-to-meter) and at rover (meter-to-submillimeter) scale, is critical for context information and for the understanding of spatial and temporal relationships in the geologic record (Mustard et al., 2013), including the in situ search of Martian biosignatures (Vago et al., 2017). Context at multiple spatial scales is needed for tactical and strategic planning of Mars rover missions and for the selection of samples to be acquired by NASA's *Perseverance* rover (operated in Jezero crater since February 2021) and to be returned to Earth during a later Mars Sample Return (MSR) mission (Mustard et al., 2013). The Approximate Scale for Images and Chemistry (ASIC) pipeline and website provides spatial scales for images from different cameras onboard NASA's *Curiosity* rover (Navcam, Mastcam, and MAHLI, Figure 1, Table 1) that cover the panoramic, hand-lens, and microscopic scales. ASIC scalebars are a simple form of planimetry and support the link between obliquely acquired landscape images and topographic and geologic maps. The major advantage of the ASIC project consists of providing spatial scale to images without requiring any specific software (except basic software for image viewing).

The top of the rover's Remote Sensing Mast (RSM, Figures 1a and 1b) carries four identical Navigation cameras (left and right, NLA/NLB and NRA/NRB, respectively, or Navcam if unspecified, Maki et al., 2012), two Mast cameras of different field of view (left and right, MR and ML, respectively, or Mastcam if unspecified, Bell et al., 2017; Malin et al., 2017), as well as the ChemCam instrument (Maurice et al., 2012; Wiens et al., 2012) that combines a Laser-Induced Breakdown Spectroscopy (LIBS) instrument and a camera, the Remote Micro-Imager (RMI, Table 1). The turret at the end of the robotic arm hosts sample handling and acquisition facilities, such as the drill and the brush, and two science instruments: the MArs Hand Lens Imager (MAHLI, Edgett et al., 2012), a focusable high-resolution color camera, and the Alpha-Particle X-ray Spectrometer (APXS, Campbell et al., 2012 and references therein) that, respectively, return macro images and the elemental composition of surface materials within the work space of the robotic arm (Figures 1c, Table 1).

Software: Walter Goetz, Michael Bruns, Stephan Thoma, Iancu Pardowitz, Thomas C. Stein
Supervision: Walter Goetz
Validation: Walter Goetz
Visualization: Walter Goetz, Stephan Thoma
Writing – original draft: Walter Goetz, Iancu Pardowitz
Writing – review & editing: Walter Goetz

The Navcam and the RMI cameras return gray-scale images. In contrast, Mastcam and MAHLI are color imagers utilizing a CCD (Charge-Coupled Device of type Kodak KAI-2020) with a Bayer pattern filter. In addition, the Mastcams are configured with narrow-band filter wheels and can therefore acquire images as part of "multispectral sequences", that is, provide spectral information at geologically and mineralogically diagnostic wavelengths across the image frame (Bell et al., 2017; Malin et al., 2017). Further information on the above-mentioned instruments can be found in Table 1 as well as in the quoted publications.

After landing of the Curiosity rover (6 August 2012) we had the idea to create a software pipeline to provide spatial scale for Mastcam and Navcam images. Later, we added MAHLI images to the pipeline, which prompted the development of a website (called the "ASIC website") to support the search for data, such as images, science targets, that is, points of scientific interest on the Martian surface, and chemical compositions of these targets, as measured by the ChemCam, and the APXS instruments. The ASIC website provides spatial scales to images as determined by the ASIC pipeline and chemical information on science targets as retrieved from NASA's data archive, the Planetary Data System (PDS). Furthermore, the website is strongly interlinked with the PDS Analyst's Notebook (AN) that provides additional information on specific images, for example, their PDS label and derived image products such as different versions of geometric or color calibration or mosaics that contain these images. A significant part of scientific and ancillary data from the mission that are communicated via AN and ASIC have actually been extracted from MSLICE (MSL Operations InterfaCE), the MSL-surface-operations planning tool.

In this paper, we describe the ASIC algorithm and the pipeline, and the process through which the scientific community can access the resource, which is now publicly available.

Obviously, ASIC-provided spatial scales are only "a start," while full 3-D information is needed for both rover operations and science analysis. In fact, a large amount of work has been done on "3-D reconstruction" (in particular "3-D Digital Outcrop Modeling") from images returned by the Mars Exploration Rovers (MER, Alexander et al., 2006; Lewis et al., 2008; Hayes et al., 2011) as well as MSL (Caravaca et al., 2021; Deen et al., 2018 and references therein). In this context the Planetary Robotics 3D (*PRo3D*) software (Balme et al., 2018; Barnes et al., 2018; Paar et al., 2018; Traxler et al., 2022) may be mentioned that has been developed for cameras onboard MER (Spirit and Opportunity), MSL, Mars-2020 (Perseverance) and ExoMars (Rosalind Franklin). *PRo3D* shall provide easy access to 3-D data of Martian surface features, allowing for example, for dip and strike measurements on sediments and 3-D rendering (see e.g., "flyover" video generated from Mastcam-Z/Mars-2020 stereo image pairs, sol 3, ASU, 2021). ASIC, however, does not attempt any form of 3-D reconstruction. In particular, the ASIC algorithm does not invoke Digital Elevation Models (DEM) that are generated from Navcam (and also Mastcam) stereo image pairs but relies entirely on simple geometric relationships for a rover assumed to move on a plane surface. Despite the simplicity of the algorithm, ASIC spatial scales enable many types of geologic and geomorphologic interpretation of rover images, and they do have sufficient accuracy for these types of analysis (see e.g., Rubin et al. (2016) and Wiens et al. (2017), where ASIC spatial scales have been used).

2. Assignment of Spatial Scale to Mastcam and Navcam Images

2.1. Algorithm and Mathematical Formalism

Mastcam and Navcam spatial scales are inferred from the viewing geometry of the respective camera and build on the fundamental assumption that the rover is standing on a plane surface (of infinite area). Hence, no DEM is invoked. The surface that the scale info is referring to, is not required to be parallel to the local Mars areoid. ASIC's spatial scale refers to features and flat-lying objects on that surface, not to rover hardware or objects with significant topographic relief (such as boulders or outcrops with steep walls). As a result of the above assumptions, ASIC cannot provide spatial scale for images of surface patches that are more than 10 m away from the rover. Deviations of the computed spatial scale from the true scale are introduced to the extent that the scene imaged by the cameras deviates from the plane defined by the ground contact of the rover wheels.

The most important task of the ASIC pipeline is to assign horizontal and vertical scalebars, that is, scalebars along pixel rows and columns, respectively, to the central-pixel column of any given Mastcam or Navcam image. Accordingly, these scalebars are termed the Central-Column ScaleBar (CCSB) and by action of the ASIC pipeline, the CCSB is displayed in a black box to the right of the image frame.

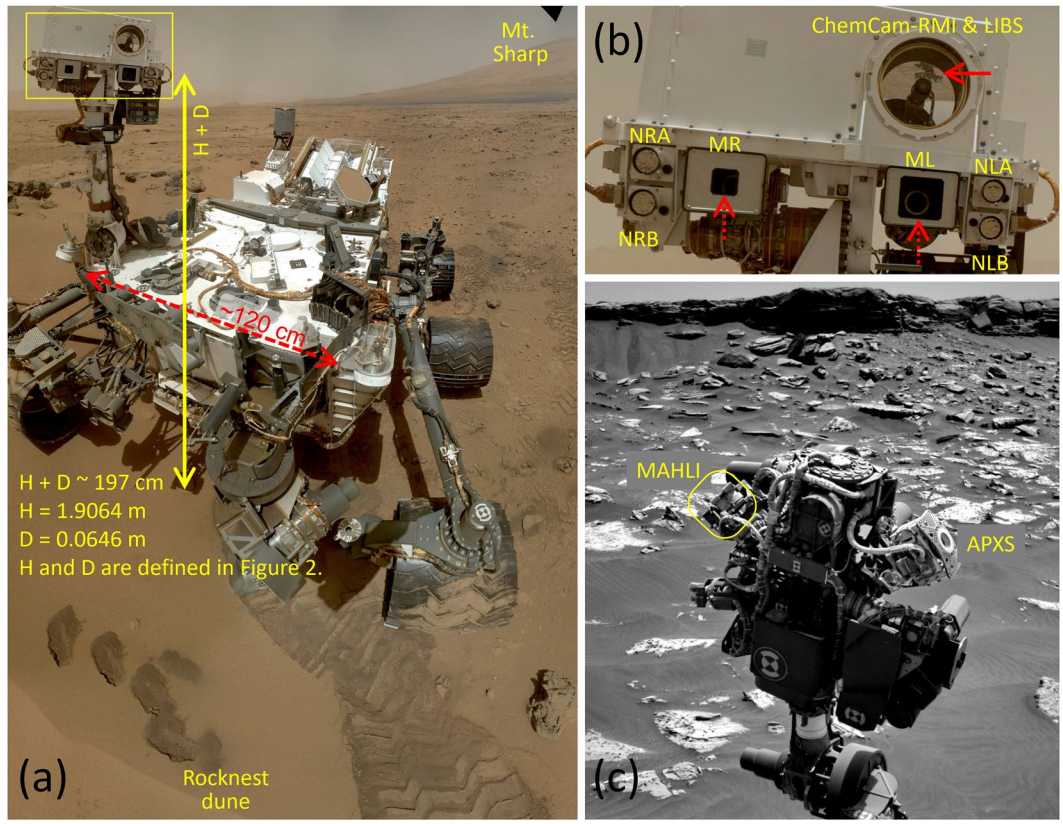

Figure 1. Instruments onboard the Curiosity rover that are relevant to this work: Cameras (Navcam, Mastcam, MAHLI, ChemCam-RMI) and analytical instruments (ChemCam-LIBS, APXS). (a) "Selfie" of the rover (acquired by MAHLI, sol 85) next to the *Rocknest* dune in Gale crater, (b) Camera head (yellow frame in a) with 2 Mastcam and 4 Navcam cameras as well as ChemCam-LIBS and ChemCam-RMI (for details see Table 1). The 2 Mastcam cameras have different field of view (Table 1) as indicated by the different size of their protective window (red dotted arrows). (c) View (NRB, sol 2740) of the turret at the end of the robotic arm with the APXS instrument and the MAHLI camera (encircled by yellow line). ChemCam uses the same telescope in order to acquire RMI images and LIBS data. Note the reflected image (in b) of the Martian landscape (upside down) and the turret (red solid arrow) in the primary mirror of the telescope. The center and lower left part of that image is obstructed by ChemCam's secondary mirror (Maurice et al., 2012; Wiens et al., 2012). *Credit: NASA, JPL, MSSS.*

The variables and parameters used by the pipeline are described in Table 2 and Figure 2. Specifically, Figures 2a and Table 2 define the angles θ_C, θ, and ϕ as well as the distances R_0, R_{CC}, and R. Figure 2b displays the (y, z)-plane ($x = 0$) of Figure 2a. Table 2 indicates that all 6 cameras (ML, MR, NLA, NLB, NRA, NRB) are assumed to be mounted at the same height on the RSM. In fact, the three stereo camera pairs NLA/NRA, ML/MR, and NLB/NRB (Figures 1a and 1b) are mounted at approximately 199 cm, 197 cm, and 194 cm, respectively, above the Martian surface (translating into three slightly different values for D,—the one given in Table 2 actually refers to Mastcam), but the error introduced by this approximation (less than 1%) is marginal as compared to the overall uncertainty of generated spatial scales.

The equations applied by the ASIC pipeline are described below. Given the "effective height" H′ of the RSM ($H' = H + D \sin(\theta_C)$), the position ($x$, y) of the projected pixel (i, j) on the (idealized) Martian surface plane can be written as (Figure 2):

$$y(\theta) = H' \tan(\theta) \tag{1}$$

$$x(\theta, \phi) = R_{CC} \tan(\phi) = \frac{H'}{\cos(\theta)} \tan(\phi) \tag{2}$$

Table 1
Instruments Onboard the Curiosity Rover That Are Relevant to This Work (Modified From Table 1 in Schieber et al., 2022)

Instrument	Short label	Category	Attributes (spatial resolution/detection limits)	Main use	Limitations
Left Navcam A (left Navigation Camera)	NLA	Visual	Image size: 1024 × 1024 pixels; FOV: 48° × 48°; image resolution: 1,640 µm pixel^{-1} at 2 m distance, 82 cm pixel^{-1} at 1 km	Geomorphology; mission planning	No color information; limited resolution
Left Navcam B	NLB	Visual	(as above)	(as above)	(as above)
Right Navcam A	NRA	Visual	(as above)	(as above)	(as above)
Right Navcam B	NRB	Visual	(as above)	(as above)	(as above)
Left Mastcam (left Mast Camera)	ML	Visual	Image size: 1600 × 1200 pixels; FOV: 20° × 15°; image resolution: 444 µm pixel^{-1} at 2 m distance, 22 cm pixel^{-1} at 1 km	Geomorphology, stratigraphy, sedimentology	Discontinuous coverage; limited points of view
Right Mastcam (right Mast Camera)	MR	Visual	Image size: 1600 × 1200 pixels; FOV: 7° × 5°; image resolution: 148 µm pixel^{-1} at 2 m distance, 7.7 cm pixel^{-1} at 1 km	(as above)	(as above)
ChemCam-RMI (Chemistry and Camera-Remote Micro-Imager)	RMI	Visual	Image: circular, 1024 pixels across; image resolution: 59 µm pixel^{-1} at 3 m distance	Stratigraphy, Sedimentology (targets at long distance), Documentation of ChemCam-LIBS targets	No color information; narrow field of view
MAHLI (Mars Hand Lens Imager)	MAHLI	Visual	Image size: 1600 × 1200 pixels; best case image resolution: 15 µm pixel^{-1}	Stratigraphy, sedimentology	Targets ≤2.5 m of rover; practical resolution limit is ca. 20 µm
APXS (Alpha Particle X-Ray Spectrometer)	APXS	Chemical	Sampled area ca. 17 mm diameter; 10 min suffice for a quick look at major elements, up to 3 hr required for all elements	Bulk rock major and trace element composition; contact instrument	Measurements take 2–3 hr to show all elements, including small amounts of trace elements
ChemCam-LIBS (laser-induced breakdown spectroscopy)	ChemCam	Chemical	Sampled area ca 0.3 mm diameter; typically 30 laser shots per ChemCam point (for good statistics) and 5 × 1 or 3 × 3 rasters	Chemical composition, remote-sensing instrument	Targets within ca 3–4 m of rover

Note. The instruments are sorted by category and spatial resolution (with lowest resolution on top).

The metric dimension of a projected pixel on the Martian surface can be derived from:

$$\Delta y = \frac{\partial y}{\partial \theta}\Delta\theta \tag{3}$$

$$\Delta x = \frac{\partial x}{\partial \phi}\Delta\phi + \frac{\partial x}{\partial \theta}\Delta\theta \tag{4}$$

Thus:

$$\Delta y = \frac{H'}{\cos^2(\theta)}\Delta\theta \tag{5}$$

$$\Delta x = \frac{H'}{\cos(\theta)\cos^2(\phi)}\Delta\phi + \frac{H'\sin(\theta)}{\cos^2(\theta)}\tan(\phi)\Delta\theta \approx \frac{H'}{\cos(\theta)\cos^2(\phi)}\Delta\phi \tag{6}$$

$$\Delta x(\phi = 0) = \frac{H'}{\cos(\theta)}\Delta\phi \tag{6a}$$

The first term in the right-hand member of Equation 6 is always dominating, especially for small elevation angles (say $\theta < 60$, 40, and 30° for MR, ML and Navcam, respectively), where the distortion due to oblique image acquisition is limited.

Table 2
Variables and Parameters Used by the ASIC Pipeline

Name	Value or range of typical values	Description
θ_C	~25° to ~85°	Camera elevation angle (off "downward")
θ_0	~5° to ~65°	Camera tilt angle, $\theta_C + \theta_0 = 90°$
θ	~20° to ~90°	Angle between (–z) axis ("downward") and R_{CC}
		Specifically: $\theta = \theta_C$ if R_{cc} points toward "center pixel"
ϕ	−3.4° to +3.4° (MR)	Azimuthal angle within Fields Of View (FOV) of Mastcam (MR and ML) and Navcam
	−10° to +10° (ML)	
	−24° to +24° (Navcam)	
$R(\theta, \phi)$	~2 to ~30 m	Distance from camera bore hole to "any pixel" on Martian surface
$R_{CC} = R(\theta, 0)$	~2 to ~30 m	Distance from camera bore hole to "any pixel along central column (cc)" on Martian surface
$R_0 = R(\theta_C, 0)$	~2 to ~20 m	Distance from camera bore hole to "center pixel' on Martian surface
H	1.9064 m	Height of mast, up to joint (elevation actuator)
D	0.0646 m	Length of top part (from joint to ML/MR boreholes) that can be tilted by angle Θ_0 so that $H' = H + D\cos\theta_0$
IFOV	0.074 mrad (MR)	Single-pixel Instantaneous Fields Of View (IFOV) of Mastcam (MR and ML) and Navcam
	0.220 mrad (ML)	
	0.820 mrad (Navcam)	

Note. The numerical range given for the variables (R_0, R_{CC}, θ_C, θ_0, θ) is actually dictated by the image selection criteria that are applied by the ASIC pipeline (Table 3, Figure 7). H, D and IFOV are fixed per rover/instrument design. Refer to Figure 2.

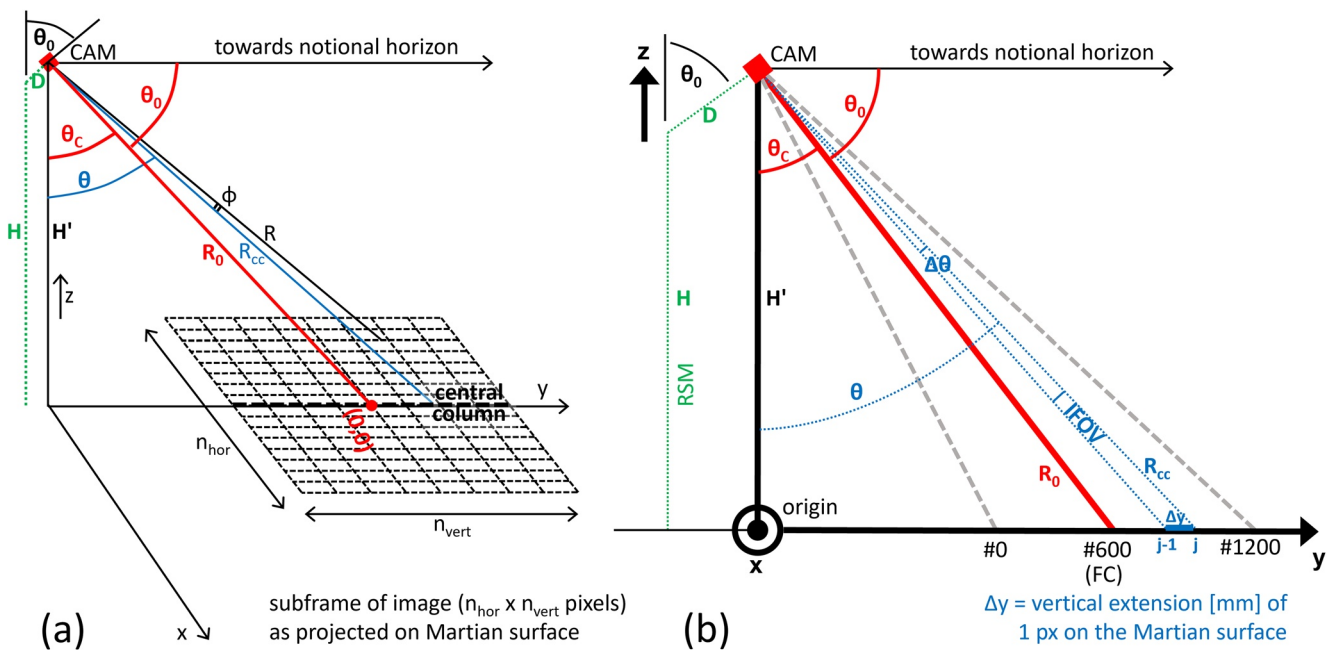

Figure 2. Variables needed to compute spatial scale for Mastcam and Navcam images. (a) 3-dimensional drawing of imaged Martian surface patch (here covered by 16 × 8 hypothetical pixels and viewing of that patch by a camera (Mastcam or Navcam). (b) Same as (a), but only showing the (y, z)-plane. The parameter j is the row number of the CCD image frame. CAM = Camera (Mastcam or Navcam). FC = Frame Center. See Table 2 for symbols and their descriptions.

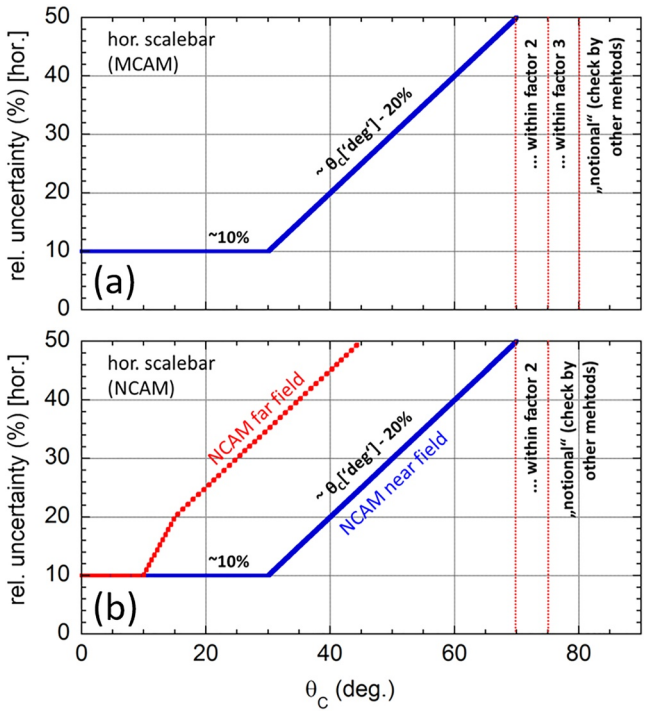

Figure 3. "Generic uncertainty" for ASIC-provided (a) Mastcam and (b) Navcam spatial scale along the horizontal direction as a function of elevation angle Θ_C (angle between the vector i.e., pointing straight down from the camera head and the camera's line of sight). The ASIC pipeline prints this uncertainty into the "info box" below each processed Navcam and Mastcam image (Figure S1 in Supporting Information S1).

In the pipeline, the "first-order' approximation of Equation 6 is used for generation of rectified images, whereas Equation 6a is used for CCSB generation.

When setting $\Delta\theta \equiv \Delta\phi \equiv$ IFOV (Instantaneous Field of View), Δx and Δy become the pixel dimensions as projected onto the Martian surface (Figure 2a). Because $\Delta y > \Delta x$ for $\theta > 0°$, the vertical resolution is worse than the horizontal resolution in terms of mm/pixel (e.g., $\Delta y \sim 0.9$ and $\Delta x \sim 0.6$ mm/px in the center of an ML image for $\theta_C = 45°$, Equations 5 and 6a). Therefore, when generating rectified images, the actual ground lengths must be taken into account to guide warping of the acquired images. Subdivision into small subframes is needed, as the distortion varies across the image frame. Usually, 16×16 px subframes were used for image processing, but the result of warping/rectification did not critically depend on the size of these subframes. For generation of rectified images, (a) the ASIC pipeline defines a reference length on the Martian surface: ref $= R_0$IFOV that is tied to the image center; (b) the pipeline subdivides the acquired image frame into small (typically 16×16 px) subframes; (c) each of the subframes is distorted along x and along y as per the Δx/ref and Δy/ref ratios, respectively. This results into horizontal contraction below the frame center (Δx/ref < 1), and expansion above center (Δx/ref > 1), and increasing vertical stretching from bottom to top of the image frame, owing to Δy/ref > 1 across the entire image.

2.2. Uncertainty of Spatial Scale

Because of the foreshortening effect along the vertical direction, deviation from the assumption of "flatness" of the terrain introduces large errors along the y axis of the image frame. Therefore, the Mastcam and Navcam spatial scales are more reliable along the horizontal rather than the vertical axis of the image. For this reason, the spatial scale along the vertical direction is characterized as "notional."

For the spatial scale along the horizontal direction, a simple scheme has been adopted that is termed "generic uncertainty" (Figure 3) and that is always printed in the black "info box" below each ASIC-processed image (Figure S1 in Supporting Information S1).

The relative generic uncertainty is defined as follows:

$$ru_{\text{generic}} = \frac{\Delta x_{\text{ASIC}} - \Delta x_{\text{true}}}{\Delta x_{\text{true}}} \tag{7}$$

The absolute values of this expression are plotted (as percentages) in Figure 3 (see also a critical discussion of these uncertainties in the Supplemental Material). Comparison of spatial scales generated by the ASIC pipeline to those inferred from stereo image pairs showed ASIC scales to be within range of the "generic uncertainties" for any terrain potentially encountered by the rover, including terrains with unusually strong topographic relief. Obviously, float rocks, boulders and other asperities of the terrain are not taken into account by the ASIC pipeline. In the particular case of a boulder, the ASIC-provided spatial scales will refer to the flat ground, the specific boulder is lying on rather than to the boulder itself, and the ASIC spatial scale will lead to an overestimation of the true size of that boulder (Figure S2 in Supporting Information S1). In general, careful visible inspection of an image may provide clues on the sign and magnitude of the error of ASIC-based sizes of objects (or any features) in the images.

2.3. Verification of Spatial Scale

Two Mastcam images are chosen to discuss the accuracy of the spatial scale as determined by the above ASIC algorithm and pipeline. Figure 4 shows the case of a left Mastcam image acquired on sol 330 (ID: mcam01336). Figures 4a and 4b show, respectively, the context map (based on an image acquired by the HiRISE camera onboard the Mars Reconnaissance Orbiter (MRO), McEwen et al., 2007) and the local context of that image (based on a mosaic of 12 ML images). Figure 4c specifies selected spatial scales (as determined from the ASIC scalebars to the right) of features of known size (as obtained by comparison with the rover components). The

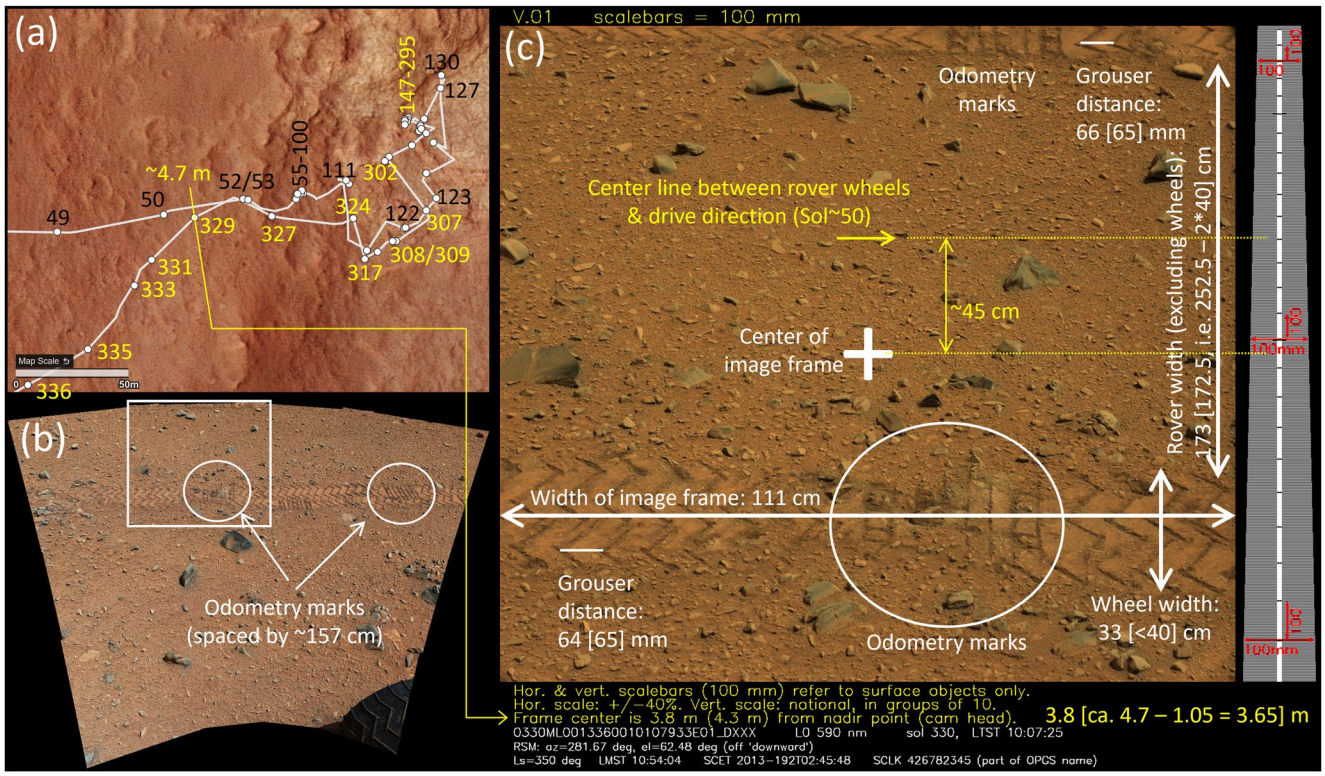

Figure 4. (a) Map of rover traverse in the sol range 49–336. The map was generated by MMGIS software (Calef et al., 2017). Sol labels are black and yellow for, respectively, way down into and way out of „Glenelg“ (note the palindromic name), the top-most stratum in the Yellowknife Bay area. (b) Mosaic of 12 ML images. (c) ML image acquired on sol 330 (0330ML0013360010107933E01, white rectangle in panel (b) of rover tracks (named ‚Letitia‘) from sol ~50. This image was acquired from the rover position that was reached on sol 329 (see panel a). It highlights different features and their associated spatial scales (both their ASIC scale and, in square brackets, their true scale [per rover design]). Note that there are two types of vertical scales: the vertical scalebars next to the image frame and the distance from rover to frame center (see “info box”). Also highlighted in panels (b and c) are the odometry marks that are spaced by ~157 cm ($\pi \times$ wheel diameter = $\pi \times 50$ cm). These odometry marks are also Morse code for „JPL“ (https://www.nasa.gov/mission_pages/msl/multimedia/pia16111.html). Credit: NASA, JPL, MSSS.

ASIC values compare very well to the “true values” (in square brackets), for example, distance between neighbor grousers on the wheels (Figure 5a), wheel width (Figure 5a), and rover width. ASIC provides two types of vertical scales, that is, distances from rover (e.g., nadir point below camera) to center of image frame (here: 3.8 m), and vertical ASIC scalebars as given to the right in Figure 4c.

Using the vertical ASIC scalebars (to the right of the image frame, Figure 4c), the width of the rover is determined to be 173 cm, which deviates from the true value (172.5 cm) by only 0.3%. The distance of 3.8 m from the camera nadir point to the frame center (see “info box”) also compares favorably to the corresponding true value (~3.65 m, rel. deviation ~4%). The latter value is obtained by subtracting the RSM offset (~60 cm to the right on the rover deck, Figure 1a) and the distance between image center and center line between rover wheels (~45 cm, Figure 4c) from the distance between sol 50 and sol 329 rover tracks (~4.7 m, Figure 4a).

The ML pointing for the image shown in Figure 4c was: rover heading +(camera azimuth—straight-ahead pointing) = 244.29° + (281.67°–181.8°) = 344.16°, that is, NNW.

This direction is indicated by a straight line in Figure 4a,—the same straight line that also has been used to determine the distance from rover position on sol 329/330 (the rover did not move on sol 330) to the wheel tracks from sol 50 (Figure 4c). The camera azimuth (az = 281.67°) in the above formula is given in the “info box” for this particular ML image (see bottom of Figure 4c) and the angle 181.8° corresponds to the “straight-ahead pointing direction” of the camera (see also Figure S1 in Supporting Information S1).

Another example demonstrating the accuracy and reliability of ASIC data products is given in Figure 5. Figure 5a, an almost ideally straight-on MAHLI image (sol 713) of the left front wheel, presents some relevant distances on the rover wheel: A and B are, respectively, the horizontal and vertical distance between two vertices of the V-shaped grouser pattern; C is the width of the wheel. Figures 5b and 5c show, respectively, the as-acquired

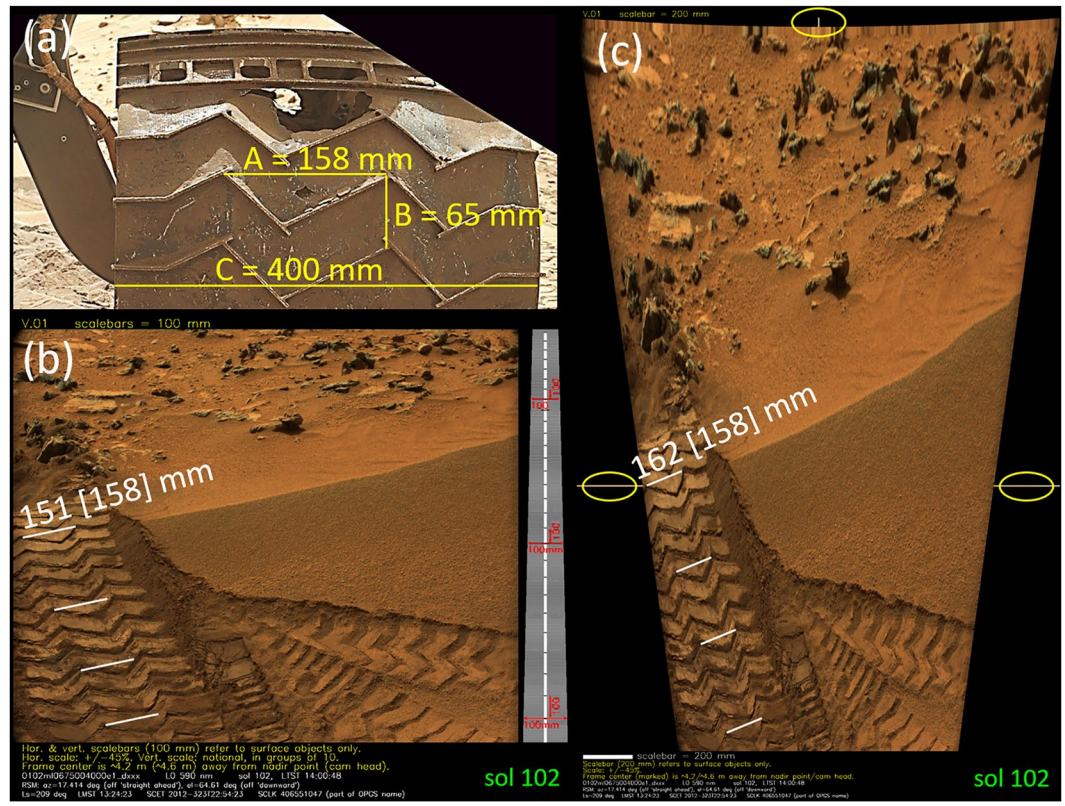

Figure 5. (a) Rover wheel metrics. MAHLI view of left front wheel (sol 713). Panels (b and c) show rover wheel tracks imprinted into the Rocknest aeolian deposit: (b) Left Mastcam image (sol 102) with central-column spatial scale to the right. (c) The same image (as in b), but rectified (warped) such that a single scalebar (here: 200 mm) applies to the entire image frame. Due to the non-linearity of image rectification, the frame center (marked by thin solid lines, see yellow circles in panel (c)) is in the lower part of the rectified image. Distances between grouser vertices ($A = 158$ mm as measured on the actual rover wheel, see panel (a)) can also be read from the grousers imprints into the soil (panels b, c). Again (as in Figure 4c) the ASIC spatial scales compare very well to the corresponding rover hardware scales (given in square brackets). Four white lines of same length have been placed in the wheel tracks in panels (b, c) and can be compared to the grouser features imprinted into the sol (see text for further details). Image ID: 0713MH0002620000204354E01 (subframe), 0102ML0006750040103027E01 (full frame). Credit: NASA, JPL, MSSS.

image (oblique) with a CCSB and its rectified (warped) version with a unique scalebar. Distance A is inferred (from Figures 5b and 5c) to be 151 and 162 mm, respectively, which is within 5% of the rover design value (158 mm, Figure 5a). Note that the value 151 mm (Figure 5b) must be inferred from the CCSB by applying the Pythagorean theorem, as the CCSB provides separate horizontal and vertical scalebars (here: 100 mm long scalebars). In this particular case, however, it would be (almost) enough in first approximation to neglect the vertical component.

In the as-acquired image shown in Figure 5b four white lines of same length have been drawn: the top one appears to connect two vertices of the V-shaped grouser pattern, whereas the others (i.e., those placed closer to the rover) do not. In its rectified version (Figure 5c) all four white lines span the same ground distance.

Because rectified images do not take into account the vertical height of real (Martian) objects (such as sand ripples or float rocks), the rectification process occasionally generates artifacts (top of Figure 5c). ASIC provides both CCSB and rectified images, if the elevation angle is less than 60° and 40° for Mastcam and Navcam, respectively (further details in following sections).

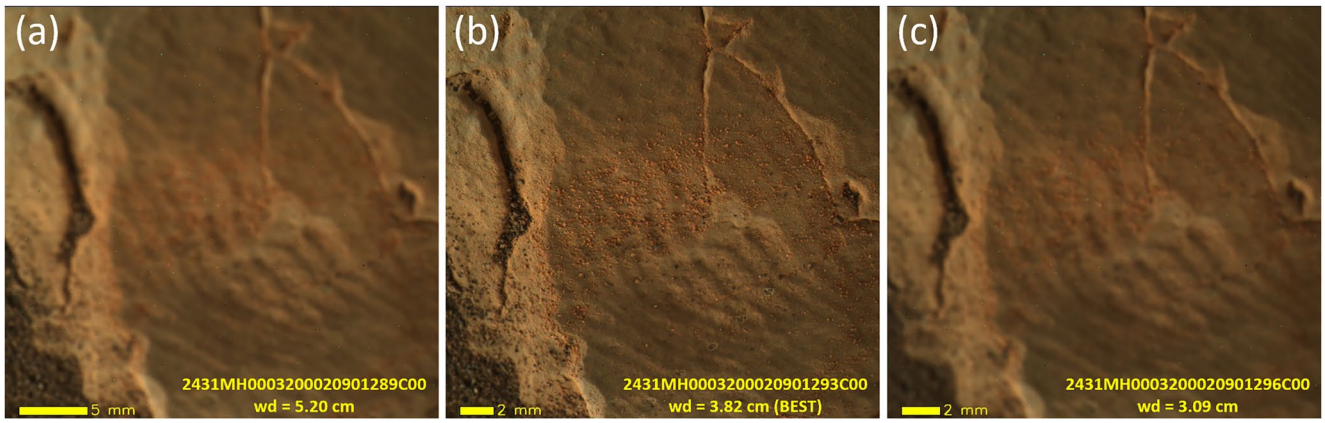

Figure 6. Example of MAHLI focus stack (sol 2431),—here shown 3 (out of 8) component images that have been acquired at different working distances ("wd," distance from MAHLI's front lens to target). Panels (a and c) show the two images that have been acquired at the most extreme working distances (5.20 and 3.09 cm, respectively) in this particular focus stack, whereas panel (b) shows the component image with best focus (wd = 3.82 cm). ASIC provides scalebars to all these component images, with the caveat that any ASIC MAHLI scalebar does only apply to in-focus images or in-focus portions of those images. Credit: NASA, JPL, MSSS.

3. Assignment of Spatial Scale to MAHLI Images

3.1. Algorithm and Mathematical Formalism

The ASIC pipeline generates scalebars for MAHLI images, provided that the working distance from MAHLI's front lens element to the imaged object is less than about 100 cm (Edgett et al., 2012). In this way, obliquely acquired MAHLI landscape images are avoided, where spatial scale varies tremendously across the image frame. A key parameter for MAHLI image acquisition is the focus motor count (fmc) that controls the position of the lens focus group inside the camera (Edgett et al., 2012). This parameter can be converted into the "working distance", that is, the distance from the camera's front lens element to the focal point in the object space (Edgett et al., 2012; Oct. 2015). We distinguish between two cases:

Case 1: IF fmc $\geq$ 12680 THEN "cover is open", working distance $\leq$ 98.05 cm and x = fmc

Case 2: IF fmc $\leq$ 4395 THEN "cover is closed", working distance $\leq$ 98.05 cm and x = 17075 – fmc (8)

Case 2 is encountered very rarely. In both cases the following formulas are applied:

$$\text{working distance (cm)} = \left[a\,x^{-1} + b + c\,x + d\,x^2 + e\,x^3\right]^{-1} \quad (9)$$

$$a = 0.576786$$

$$b = -11.8479$$

$$c = 2.80153\,10^{-3}$$

$$d = -2.266488\,10^{-7}$$

$$e = 6.26666\,10^{-12}$$

$$\text{pixel scale}\,(\mu\text{m/px}) = 6.9001 + 3.5201 \times \text{working distance (cm)} \quad (10)$$

Equations 8, 9, and 10 are from, respectively, 4, 3 and 2 in Edgett et al. (Oct. 2015, pp. 24–29). Examples of application of these formulas are shown in Figure 6 and Figure S3 in Supporting Information S1 (the latter Figure belonging to the Supplemental Material).

3.2. Uncertainty

For MAHLI focus merge products (the so-called "R-type images," see Appendix A), ASIC capabilities are limited, because the header does not provide sufficient information for the computation of an average pixel scale. Thus, presently the ASIC pipeline does avoid MAHLI Z-stack focus merge (R-type) images but provides spatial

Table 3
Image Selection Criteria of the ASIC Pipeline for Mastcam, Navcam and MAHLI Images

Camera	ASIC selection criteria
Mastcam	i) Images of type C, E or F
	ii) Image size: ≥1,000 columns and ≥1,000 rows
	iii) Elevation angle: $\theta_C \leq 85°$ (See Figure 7)
Navcam	i) EDR images
	ii) Image size: ≥1,000 columns and ≥1,000 rows
	iii) Elevation angle: $\theta_C \leq 85°$ (See Figure 7)
MAHLI	i) Images of type C, E or F
	ii) Image size: ≥256 columns and ≥256 rows
	iii) Images *not* from sol 274 (MAHLI focus check campaign)
	iv) Working distance: wd < 1 m (avoid landscape images with focus at infinity)

Note. The criteria specified for each camera must all be met simultaneously. Meeting the Mastcam and Navcam criteria does not necessarily imply generation of an image with scalebar (see Figure 7).

scale for all individual component images which are usually of C-type (single image, lossless compression, see Appendix A): if the particular C-type image considered is in focus, then the ASIC-provided scalebar can be considered to be valid. If only a small subframe of an image is in focus, the scalebar applies only to that particular subframe. Presently, ASIC does not include an algorithm for automatic identification of out-of-focus imagery. Figure 6 shows three (out of eight) component images of a MAHLI Z-Stack: 2431MH0003200020901**289**C00 (Figure 6a) through …**296**C00 (Figure 6c), with …**293**C00 (Figure 6b) being the sharpest image in this Z-Stack series. The relative deviation of spatial scales for the two extreme images (Figures 6a and 6c) from the one for the best-focus image (Figure 6b) is about 17%. Obviously, direct comparison of differently focused images helps to identify the image that is "mostly in focus" (considering the entire frame). However, the two extreme images shown in Figures 6a and 6c are immediately identified as being out of focus (again: with their scalebars being in error by about 17%). Therefore, we argue that "average human vision" will allow to discriminate between in-focus and "slightly out-of-focus" images, such that ASIC-inferred scalebars for MAHLI images are accurate to within 10%. This statement is supported by the additional check of ASIC-provided spatial scales for objects of known size (such as the US penny and drill holes, see also Figure S3 in Supporting Information S1). The scale of any R-type image should therefore be equal (within 10% accuracy) to the scale of the "best" Z-Stack component

angle θ_C	action by ASIC Software on MCAM & NCAM images
$\theta_C > 85°$	image is ignored (see Table 2)
$0° \leq \theta_C \leq 85°$	"_raw_scale" or "_raw_noscale" (suffix added to the image filename) is generated, depending on the code's dynamic decision:
	CCSB is only drawn up to θ = 75° (see panel to the right).
	IF there is space for three or more vertical scalebars[a], THEN "raw_scale" (with CCSB) is generated, ELSE "raw_noscale" is generated, where the notional distance from rover to frame center ('info box') provides a 'sense of scale'. These cases are illustrated by the panels to the right. [a]True, if $\theta_C < 76.6°$, 80.3° and 83.5° (approximate values for MR, ML and NCAM, respectively)
$0° \leq \theta_C \leq 60°$ [MCAM]	"rectified" is generated (scalebar & grid). See example in Figure 3c.
$0° \leq \theta_C \leq 40°$ [NCAM]	

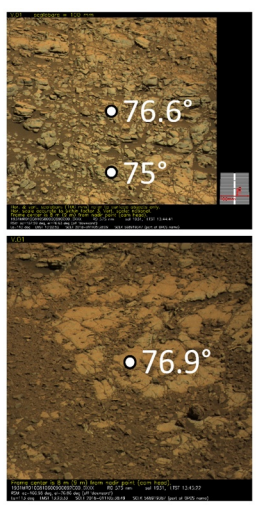

Figure 7. Processing of Mastcam and Navcam images by the ASIC pipeline as a function of the elevation angle θ_C. Distinguish between the angles θ_C and θ (see Table 2, Figure 2). An alternative overview of ASIC data products is given in Figure S1 in Supporting Information S1. Image ID: 1931MR0100810580900690C00, $\theta_C = 76.63°$. 1931MR0100810600900692C00, $\theta_C = 76.86°$. Credit: NASA, JPL, MSSS.

image (as judged by visual inspection), although for (above explained) technical reasons, ASIC cannot display scalebars in focus-merge images. The latter type of image can also be generated onboard without downloading the individual component images, and in that case the scale for this MAHLI target is not available in ASIC. In summary, ASIC MAHLI scalebars are accurate to within 10% and should always be understood to indicate the scale of in-focus elements of images that are not focus merge products. In some cases, however, this rule may be difficult to apply (see Figure S3 and related discussion in Supporting Information S1).

4. ASIC Pipeline: Selection and Processing of Images

The ASIC pipeline ingests Navcam, Mastcam and MAHLI images according to the selection criteria listed in Table 3. These images are essentially of EDR type (Experiment Data Record), that is, they have been edited for science use, but have not been subjected to any other processing (EDR data are also referred to as NASA Level 0, Bell et al., 2017). Only minimal image processing is performed: (a) 8-to-11-bit "decompanding" on Mastcam and MAHLI images, since these images have been "companded" from 11 to 8 bit prior to download from Mars to Earth (Bell et al., 2017; for Navcam images this step is omitted since they are already downloaded with 12 bit dynamic range (Maki et al., 2012 and references therein)), and (b) mild stretching of Mastcam and MAHLI images between lowest and highest DN and slightly enhanced stretching of Navcam images (stretching between lowest and highest DN after removal of 1% darkest and 1% brightest pixels).

The ASIC software processes all types of Navcam images as well as C-, E-, and F-type images that have been acquired by Mastcam and MAHLI. C-type images are lossless compressed and E- and F-type images are in JPEG format (see Appendix A and Bell et al., 2017 for further details). Only very few MAHLI images throughout the entire mission have been encoded and transmitted in D format (JPEG grayscale, see Appendix A), while Mastcam D-type images are numerous, as they are acquired for "sky flats", that is, images of the sky in order to monitor the flat-field response of the camera, including dust settling on the protective window), imaging of astronomical objects (e.g., Phobos and Deimos) and, in most cases, as part of multispectral sequences (see Introduction). However, they are generally of lower spatial resolution than Bayer-filter Red-Green-Blue images (hereafter referred to as RGB images, acquired through the broadband filters, L0 and R0, of the Mastcam filter wheels, Bell et al., 2017), and do not contribute to the main goal of the ASIC project that is centered on high-resolution color images, that is, spatial scale, color, morphology and texture of imaged surface features as well as their chemical information. More importantly, whenever a multispectral Mastcam-sequence was commanded, an RGB image has been taken as well. Therefore D-type images are listed in the "Target Search" area of the ASIC website (see Section 5), but are otherwise not shown in ASIC. In particular, D-type Mastcam images are not processed in terms of spatial scale.

It should be apparent from the mathematical formalism (Section 2) that ASIC scalebars cannot be obtained for Mastcam and Navcam images approaching or containing the (notional) horizon. These images are often subframed (typically to less than 1,000 rows) and are therefore excluded from ASIC image processing (Table 3). For the same reason, spatial scale (CCSB) is only provided for Navcam and Mastcam images, if their elevation angle $\theta_C \leq 85°$ (Table 3, Figure 7). Moreover, no CCSB is drawn beyond $\theta = 75°$ (see example in Figure 7) which corresponds to a distance of 7–8 m from the rover. Additionally, it was not deemed worthwhile to provide scalebars to images with only a few pixel rows near the bottom of the image satisfying the condition for $\theta \leq 75°$. The transition from images with CCSB to those without CCSB is handled dynamically by the ASIC pipeline (Figure 7): images with $\theta_C < 76.6°$, 80.3°, and 83.5° (approximate values) for MR, ML and Navcam, respectively, will be provided with either a full or a partial CCSB (given condition $\theta \leq 75°$, Figure 2).

5. ASIC Website: Synoptic of Images, Spatial Scale and Chemical Composition

The ASIC website provides access to all data products generated by the above-described pipeline and, in addition, it provides access to all (or most) science targets and their chemical compositions. The website (Figure 8) has two domains ("tabs") to search for data: *ASIC Home* and *ASIC TargetSearch*.

ASIC Home (Figure 8a) provides access to all ASIC-processed Mastcam, Navcam and MAHLI images according to 6 search criteria (parameter ranges in parentheses): season L_S (0–360°), Local True Solar Time (LTST, 12:00 a.m.–11:59 p.m.), sol number (integer >0), Spacecraft Clock Time (SCLK, long integer >397504830), azimuth angle (0–6.32 rad), elevation angle (0.14–1.49 rad).

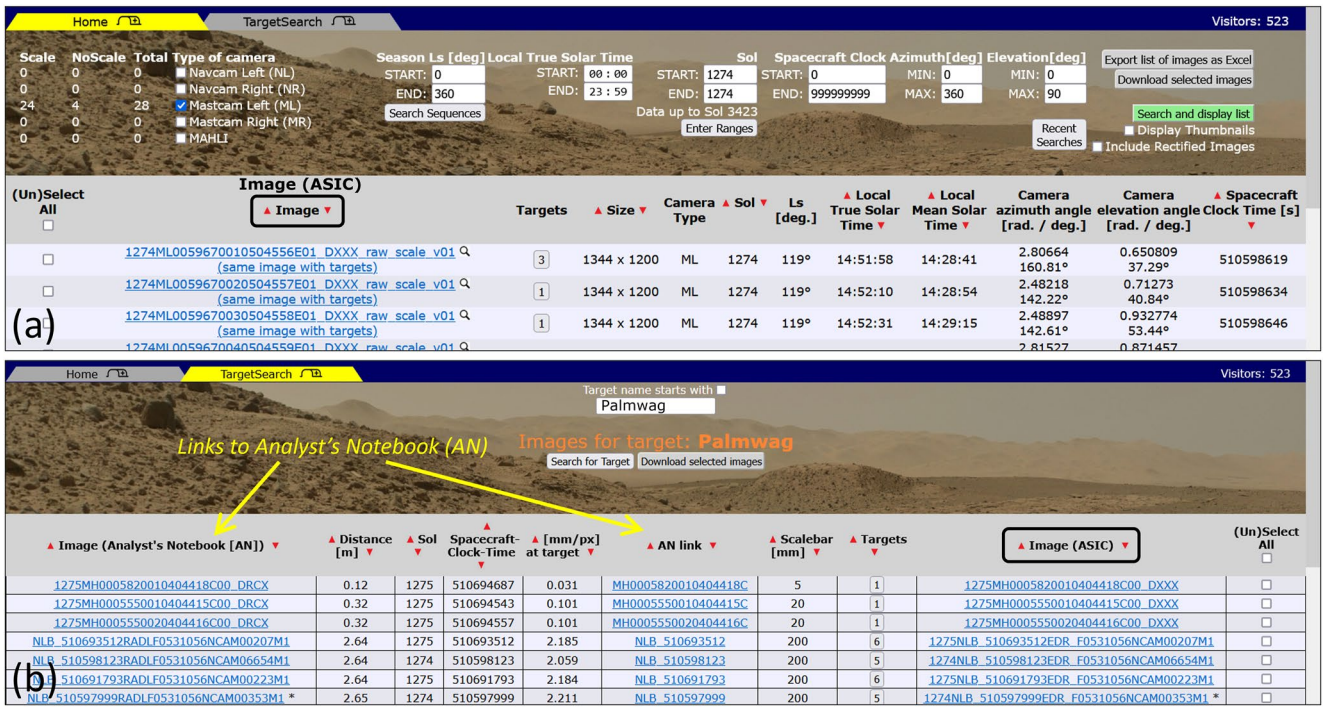

Figure 8. The ASIC website. (a) The "ASIC Home" domain: search for images throughout the mission, according to season, Local True Solar Time, sol (here: sol 1274), Spacecraft Clock Time, camera azimuth, camera elevation, and display the results of this search. (b) The "ASIC TargetSearch" domain: search a target (here: "Palmwag', sols 1274–1275) and list all images that do show this target (within max. 50 m from the rover). Two columns contain links to the Analyst's Notebook. An expanded version of this figure can be found in Supporting Information S1 (Figure S8).

ASIC TargetSearch (Figure 8b) allows to search for any specific science target. Search results will be Navcam, Mastcam and MAHLI images with/without spatial scale, where that specific target is visible. Additionally, *ASIC TargetSearch* provides access (via direct hyperlinks) to higher-level calibrated image data in the Planetary Data System Analyst's Notebook (AN) that have been linearized, radiation-corrected and/or color-corrected by the respective instrument teams (Bell et al., 2017; Maki et al., 2012; Malin et al., 2017). The AN (https://an.rsl.wustl.edu) is a web application that offers access to peer-reviewed, released data integrated with documentation describing context for observations, processing methodology, and data formats from Curiosity rover surface operations. There are two types of hyperlinks from ASIC *TargetSearch* to the AN (Figure 8b): a direct link to a specific 2%-stretched image and another link to the AN product detail page for that specific image, where the higher-level calibrated color image (the DRCX-type data product, Bell et al., 2017; Malin et al., 2017) can be downloaded either in PNG or JPEG format or in PDS archive format. In addition, the AN detail page includes image metadata and additional image product types.

The ASIC pipeline and the AN use the same set of science targets, extracted from the MSLICE planning tool used by the science team to define targets. Each target's location information includes ground coordinates relative to the rover and its position on a finder frame from which other images of a target can be auto-located. The AN auto location function is limited to finding images acquired within 50 m of a target. The AN includes a downloadable science target summary table and a target search function. In addition, the image measurement tool may be used to annotate images with targets.

Both the *ASIC Home* and *ASIC TargetSearch* tabs provide access to ChemCam-LIBS and APXS data on chemical composition of all science targets analyzed by either one of these (or both) instruments: Upon hovering with a computer mouse above some target, the chemical compositions pop up immediately as retrieved from the PDS. Additionally, a more detailed chemical data table is available displaying the chemical composition of that same (Martian) target next the ones of terrestrial reference samples that are used for calibration of the Martian data (Clegg et al., 2017; Wiens et al., 2013). In addition to the above-mentioned image types (Mastcam, Navcam, MAHLI), also ChemCam-RMI images (Remote Micro-Imager) of ChemCam targets and the context and contour MR images of ChemCam targets can be retrieved. More detailed information on the ASIC website and an expanded version of Figure 8 can be found in the Supplemental Material.

6. Summary and Outlook

An algorithm for determining the spatial scale in images (Mastcam, Navcam) acquired by Mars rovers has been presented. Its fundamental assumption is that the rover is standing on an infinite plane surface that is level or not with respect to the local Martian areoid. Spatial scales are inferred from the inclination of the cameras (Mastcam, Navcam) as key parameter,—given the design parameters of the rover's Remote Sensing Mast and the cameras (Mastcam, Navcam) on top of that mast. A software pipeline processes Mastcam and Navcam images acquired within a 20 m radius and determines the spatial scales of features that are located within 10 m from the rover. The key feature of the pipeline is that it only uses data from the label (image metadata) saved together with any particular image in the PDS archive. Thus, the pipeline requires no other information or ancillary data sets. Specifically, algorithm and pipeline do not invoke Digital Elevation Models that are inferred either from rover stereo images (acquired by ML and MR, NL and NR) or from orbital stereo images (e.g., acquired by HiRISE). This has the advantage that inferred spatial scales lack artifacts (e.g., gaps in the terrain mesh) and are always consistent. As for any other scientific data set, it is important to keep the limitations of ASIC spatial scales in mind: Whenever some object is significantly sticking out of the ideal plane surface, on which the rover is standing and roving, the size of that object may be overestimated (see Figure S2 in Supporting Information S1).

Obviously, the ASIC algorithm can be easily applied to any mast camera onboard any Mars rover. In the frame of the *ASIC* project and pipeline, the algorithm is continuously being applied to images acquired by both wide-angle (engineering) cameras (Navcam, FOV ∼48°) and narrow-angle cameras (ML and MR, FOV ∼20° and 7°, respectively) on the top of Curiosity's Remote Sensing Mast (RSM). Comparison to features of known size (e.g., drill holes, rover wheel tracks) demonstrates that the true uncertainties on spatial scale (as derived from the *ASIC* algorithm) are clearly better than the generic ones that are automatically given below each processed image, especially for images acquired by the narrow-angle cameras. The ASIC pipeline does also determine spatial scale for MAHLI images, although the underlying algorithm is based on the focus motor count, that is, one of MAHLI's image acquisition parameters, and is thus totally different from the one used for Mastcam and Navcam images. MAHLI spatial scale is provided for in-focus objects that are less than 1 m away from MAHLI's front lens element.

Finally, the *ASIC* website (https://asic.mps.mpg.de) has been created in order to combine spatial scale of objects and targets on the Martian surface with high-resolution color images and information on chemical composition and to provide easy access to all these data. The *ASIC* website is intimately linked to Analyst's Notebook (AN, https://an.rsl.wustl.edu) such that all (or nearly all) surface images of the mission can be accessed as ASIC image (with scalebar) and/or as radiometrically calibrated/linearized Navcam or color-corrected Mastcam/MAHLI image. Moreover, all science targets and their (approximate) positions in images (as retrieved from Curiosity's planning software tool MSLICE) are displayed in both ASIC and AN. In summary, ASIC is a dynamic (continuously updated) website that—interlinked with and complementary to AN—will hopefully stimulate scientific work with Curiosity's images and chemical data worldwide.

Appendix A: Types of Raw and Processed Mastcam Images

Table A1 is an excerpt from Table 3 (modified) in Bell et al. (2017). The image type is usually the third last character of the image ID string. Image types C, D, E, F, and I exist for both Mastcam and MAHLI, while images types R and T are reserved for MAHLI.

Table A1
Types of Raw and Processed Images That Can Be Generated by the Mastcam (ML and MR) and MAHLI Cameras (Bell et al., 2017)

Type	Form	Encoding
C	Image (Mastcam, MAHLI)	Losslessly compressed (Huffman)
D	Image (Mastcam, MAHLI)	JPEG grayscale (luminance only)
E	Image (Mastcam, MAHLI)	JPEG 4:2:2 YCrCb chrominance subsampling
F	Image (Mastcam, MAHLI)	JPEG 4:4:4 YCrCb chrominance subsampling
I	Image Thumbnail (Mastcam, MAHLI)	JPEG 4:4:4 YCrCb chrominance subsampling
R	Focus Merge Image (from ZStack, MAHLI)	JPEG 4:4:4 YCrCb chrominance subsampling
T	Focus Merge Thumbnail (MAHLI)	JPEG 4:4:4 YCrCb chrominance subsampling

Data Availability Statement

The ASIC website can be accessed via https://asic.mps.mpg.de. The core part of ASIC includes non-rectified images with central-column scalebar, science targets and chemical data (APXS, ChemCam) as available in the PDS archive. The ASIC website is strongly interlinked with Analyst's Notebook (https://an.rsl.wustl.edu/msl), and a very large number of specific hyperlinks (within ASIC) point directly to data residing in Analyst's Notebook. In addition, the following (external) data products can be accessed from within ASIC: Chemical composition of ChemCam science targets (Wiens, 2013a): http://pds-geosciences.wustl.edu/msl/msl-m-chemcam-libs-4_5-rdr-v1/mslccm_1xxx/data/moc. Mosaics of high-resolution grey-scale images of ChemCam science targets (Wiens, 2013b): http://pds-geosciences.wustl.edu/msl/msl-m-chemcam-libs-4_5-rdr-v1/mslccm_1xxx/extras/rmi_mosaics. The component images have been acquired by ChemCam's RMI (Remote Micro-Imager). Mastcam context color images of ChemCam science targets: http://pds-geosciences.wustl.edu/msl/msl-m-chemcam-libs-4_5-rdr-v1/mslccm_1xxx/extras/rmi_contours_in_mcam_images. Chemical composition of APXS science targets (Gellert, 2013): http://pds-geosciences.wustl.edu/msl/msl-m-apxs-4_5-rdr-v1/mslapx_1xxx/extras.

Acknowledgments
The early development of ASIC benefitted significantly from DFG Grant GO 2288/1-1 (Deutsche Forschungsgemeinschaft) that allowed one of us (WG) to participate in the primary phase of the Curiosity rover mission at the Jet Propulsion Laboratory (Pasadena, August through November 2012). During that time, Morten Bo Madsen (MBM), Copenhagen University, has been closely involved in formulating the initial idea and requirements of ASIC. Specifically, the analysis of clasts early during the Curiosity mission (Yingst et al., 2013) has been motivating the development of a simple algorithm to associate spatial scale to images on a pipeline basis. In the years 2013–2014 an early version of the ASIC pipeline was maintained and executed at Univ. Copenhagen under the supervision of MBM. Thereby, Univ. Copenhagen has played a key role in maintaining the momentum of the ASIC project. Matthew Heverly, JPL, has provided some dimensions of the Curiosity rover and its mechanical subsystems (especially the wheels) that were used to assess and demonstrate the accuracy of spatial scale in Martian landscape images as determined by the ASIC pipeline (see Figures 1, 4, and 5 in the present manuscript). James F. Bell, Arizona State University (ASU) has influenced several stages of ASIC development, including the design of the CCSB (Central-Column ScaleBars), and, not least, he encouraged us to write this manuscript for *Earth and Space Science*. Ernest Cisneros (ASU) helped in resolving ASIC pipeline problems in 2020. The integration of MAHLI images, a late step of ASIC development, has been supported by Kenneth S. Edgett, Malin Space Science Systems (MSSS), San Diego. Finally, we are grateful for the outstanding initial work on this very manuscript by Peter Fox, former editor of this journal (deceased 27 March 2021), two thoughtful reviews by, respectively, Roger C. Wiens, Purdue University, and an anonymous reviewer, and the careful reshaping of the entire manuscript by Graziella Caprarelli, current editor of this journal. Open Access funding enabled and organized by Projekt DEAL.

References

Alexander, D. A., Deen, R. G., Andres, P. M., Zamani, P., Mortensen, H. B., Chen, A. C., et al. (2006). Processing of Mars Exploration Rover imagery for science and operations planning. *Journal of Geophysical Research*, *111*(E2), E02S02. https://doi.org/10.1029/2005JE002462

ASU. (2021). Retrieved from https://live-mastcamz.ws.asu.edu/first-3-d-mastcam-z-team-flyover-of-perseverances-vicinity-assembled-from-publicly-released-stereo-products/ or https://www.youtube.com/watch?v=_340_h15xag

Balme, M., Robson, E., Barnes, R., Butcher, F., Fawdon, P., Huber, B., et al. (2018). Surface-based 3D measurements of small Aeolian bedforms on Mars and implications for estimating ExoMars rover traversability hazards. *Planetary and Space Science*, *153*, 39–53. https://doi.org/10.1016/j.pss.2017.12.008

Barnes, R., Gupta, S., Traxler, C., Ortner, T., Bauer, A., Hesina, G., et al. (2018). Geological analysis of Martian rover-derived digital outcrop models using the 3-D visualization tool, planetary robotics 3-D viewer—Pro3D. *Earth and Space Science*, *5*(7), 285–307. https://doi.org/10.1002/2018EA000374

Bell, J. F., III., Godber, A., McNair, S., Caplinger, M. A., Maki, J. N., Lemmon, M. T., et al. (2017). The Mars Science Laboratory Curiosity rover Mastcam instruments: Preflight and in-flight calibration, validation, and data archiving. *Earth and Space Science*, *4*(7), 396–452. https://doi.org/10.1002/2016EA000219

Calef, F. J., III., Gengl, H. E., Soliman, T., Abercrombie, S. P., & Powell, M. W. (2017). MMGIS: A multi-mission geographic information system for insitu Mars operations, 47th LPSC (p. 2541). Retrieved from https://www.hou.usra.edu/meetings/lpsc2017/pdf/2541.pdf

Campbell, J. L., Perrett, G. M., Gellert, R., Andrushenko, S. M., Boyd, N. I., Maxwell, J. A., et al. (2012). Calibration of the Mars Science Laboratory alpha particle X-ray spectrometer. *Space Science Reviews*, *170*(1–4), 319–340. https://doi.org/10.1007/s11214-012-9873-5

Caravaca, G., Le Mouélic, S., Rapin, W., Dromart, G., Gasnault, O., Fau, A., et al. (2021). Long-distance 3D reconstructions using photogrammetry with curiosity's ChemCam remote micro-imager in gale crater (Mars). *Remote Sensing*, *13*(20), 4068. https://doi.org/10.3390/rs13204068

Clegg, S. M., Wiens, R. C., Anderson, R. B., Forni, O., Frydenvang, J., Lasue, J., et al. (2017). Recalibration of the Mars Science Laboratory ChemCam instrument with an expanded geochemical database. *Spectrochimica Acta B*, *129*, 64–85. https://doi.org/10.1016/j.sab.2016.12.003

Deen, R. G., Abarca, H. E., Algermissen, S. S., Maki, J. N., Ruoff, N. A., Culver, A. D., et al. (2018). MASTCAM stereo analysis and mosaics (MSAM), 48th LPSC (p. 2332). Retrieved from https://www.hou.usra.edu/meetings/lpsc2018/pdf/2332.pdf

Edgett, K. S., Caplinger, M. A., Maki, J. N., Ravine, M. A., Ghaemi, F. T., McNair, S., et al. (2015). Curiosity's robotic arm-mounted Mars Hand Lens Imager (MAHLI): Characterization and calibration status. *MSL MAHLI Technical Report 0001, version 2*. https://www.researchgate.net/publication/282575409_Corrected_version_2_of_-_Curiosity's_robotic_arm-mounted_Mars_Hand_Lens_Imager_MAHLI_Characterization_and_calibration_status

Edgett, K. S., Yingst, R. A., Ravine, M. A., Caplinger, M. A., Maki, J. N., Ghaemi, F. T., et al. (2012). Curiosity's Mars hand lens imager (MAHLI) investigation. *Space Science Reviews*, *170*(1–4), 259–317. https://doi.org/10.1007/s11214-012-9910-4

Gellert, R. (2013). Mars Science Laboratory Alpha Particle X-ray spectrometer RDR data V1.0 (MSL-M-APXS-4/5-RDR-V1.0) [Dataset]. NASA Planetary Data System. https://doi.org/10.17189/1519440

Hayes, A. G., Grotzinger, J. P., Edgar, L. A., Squyres, S. W., Watters, W. A., & Sohl-Dickstein, J. (2011). Reconstruction of Eolian bed forms and paleocurrents from cross-bedded strata at Victoria Crater, Meridiani Planum Mars. *Journal of Geophysical Research: Planets*, *116*, E00F21. https://doi.org/10.1029/2010JE003688

Lewis, K. W., Aharonson, O., Grotzinger, J. P., Squyres, S. W., Bell, J. F., III., Crumpler, L. S., & Schmidt, M. E. (2008). Structure and stratigraphy of Home plate from the spirit Mars exploration rover. *Journal of Geophysical Research*, *113*(E12), E12S36. https://doi.org/10.1029/2007JE003025

Maki, J., Thiessen, D., Pourangi, A., Kobzeff, P., Litwin, T., Scherr, L., et al. (2012). The Mars Science Laboratory engineering cameras. *Space Science Reviews*, *170*(1–4), 77–93. https://doi.org/10.1007/s11214-012-9882-4

Malin, M. C., Ravine, M. A., Caplinger, M. A., Tony Ghaemi, F., Schaffner, J. A., Maki, J. N., et al. (2017). The Mars Science Laboratory (MSL) mast cameras and descent imager: Investigation and instrument descriptions. *Earth and Space Science*, *4*(8), 506–539. https://doi.org/10.1002/2016EA000252

Maurice, S., Wiens, R. C., Saccoccio, M., Barraclough, B., Gasnault, O., Forni, O., et al. (2012). The ChemCam instrument suite on the Mars Science Laboratory (MSL) Rover: Science objectives and mast unit description. *Space Science Reviews*, *170*(1–4), 95–166. https://doi.org/10.1007/s11214-012-9912-2

McEwen, A. S., Eliason, E. M., Bergstrom, J. W., Bridges, N. T., Hansen, C. J., Delamere, W. A., et al. (2007). Mars reconnaissance orbiter's High Resolution Imaging Science Experiment (HiRISE). *Journal of Geophysical Research*, *112*(E5), E05S02. https://doi.org/10.1029/2005JE002605

Mustard, J. F., Adler, M., Allwood, A., Bass, D. S., Beaty, D. W., Bell, J. F., et al. (2013). Report of the Mars 2020 science definition team. https://mepag.jpl.nasa.gov/reports/MEP/Mars_2020_SDT_Report_Final.pdf

Paar, G., Barnes, R., Gupta, S., Traxler, C., Gunn, M., & Koeberl, C. (2018). Validation of the 3D vision and visualization frameworks PRoViP and PRo3d for the Mars2020 and ExoMars stereo panoramic camera systems, 48th LPSC, 2688. https://www.hou.usra.edu/meetings/lpsc2018/pdf/2688.pdf

Rubin, D. M., Fairén, A. G., Martínez-Frías, J., Frydenvang, J., Gasnault, O., Gelfenbaum, G., et al. (2016). Fluidized sediment pipes in Gale crater, Mars, and possible Earth analogs, Geology. *Geology*, *45*(1), 7–10. https://doi.org/10.1130/G38339.1

Schieber, J., Bohacs, K. M., Coleman, M., Bish, D., Reed, M. H., Thompson, L., et al. (2022). Mars is a mirror – Understanding the Pahrump hills mudstones from a perspective of Earth analogues, sedimentology. *Sedimentology*, *69*(6), 2371–2435. https://doi.org/10.1111/sed.13024

Traxler, C., Ortner, T., Hesina, G., Barnes, R., Gupta, S., Paar, G., et al. (2022). The PRoViDE framework: Accurate 3D geological models for virtual exploration of the Martian surface from rover and orbital imagery, Chapter 3. In (Eds.), A. Bistacchi, M. Massironi, & S. Viseur (Eds.), *Digital geological models: From terrestrial outcrops to planetary surfaces* (Vol. 3D). John Wiley & Sons, Inc. https://doi.org/10.1002/9781119313922.ch3

Vago, J. L., Westall, F., Pasteur Instrument Teams, Landing S, Coates, A. J., Jaumann, R., Korablev, O., et al. (2017). Habitability on early Mars and the search for biosignatures with the ExoMars rover. *Astrobiology*, *17*(6–7), 471–510. https://doi.org/10.1089/ast.2016.1533

Wiens, R. C. (2013a). MSL ChemCam laser induced breakdown spectrometer derived data V1.0 (MSL-M-CHEMCAM-LIBS-5-RDR-V1.0) [Dataset]. NASA Planetary Data System. https://doi.org/10.17189/1519485

Wiens, R. C. (2013b). MSL ChemCam remote micro- imaging camera raw data V1.0 (MSL-M-CHEMCAM-RMI-5-RDR-V1.0) [Dataset]. NASA Planetary Data System. https://doi.org/10.17189/1519494

Wiens, R. C., Maurice, S., Barraclough, B., Saccoccio, M., Barkley, W. C., Bell, J. F., et al. (2012). The ChemCam instrument suite on the Mars Science Laboratory (MSL) rover: Body unit and combined system tests. *Space Science Reviews*, *170*(1–4), 167–227. https://doi.org/10.1007/s11214-012-9902-4

Wiens, R. C., Maurice, S., Lasue, J., Forni, O., Anderson, R. B., Clegg, S., et al. (2013). Pre-flight calibration and initial data processing for the ChemCam laser-induced breakdown spectroscopy instrument on the Mars Science Laboratory rover. *Spectrochimica Acta Part B At. Spectrosc*, *82*, 1–27. https://doi.org/10.1016/j.sab.2013.02.003

Wiens, R. C., Rubin, D. M., Goetz, W., Fairén, A. G., Schwenzer, S. P., Grotzinger, and the MSL science team, et al. (2017). Centimeter to decimeter spherical shells and voids in Gale crater sediments, Mars. *Icarus*, *289*, 144–156. https://doi.org/10.1016/j.icarus.2017.02.003

Yingst, R. A., Kah, L. C., Palucis, M., Williams, R. M. E., Garvin, J., Bridges, J. C., et al. (2013). Characteristics of pebble and cobble-sized clasts along the Curiosity rover traverse from Bradbury Landing to Rocknest. *Journal of Geophysical Research: Planets*, *118*(11), 2361–2380. https://doi.org/10.1002/2013JE004435

References From the Supporting Information

Anderson, R. C., Jandura, L., Okon, A. B., Sunshine, D., Roumeliotis, C., Beegle, L. W., et al. (2012). Collecting samples in Gale crater, Mars: An overview of the Mars Science Laboratory sample acquisition, sample processing and handling system. *Space Science Reviews*, *170*(1–4), 57–75. https://doi.org/10.1007/s11214-012-9898-9

Berger, J. A., King, P. L., Gellert, R., Campbell, J. L., Boyd, N. I., Pradler, I., et al. (2014). MSL-APXS titanium observation tray measurements: Laboratory Experiments and results for the rocknest fines at the curiosity field site in Gale crater, Mars. *Journal of Geophysical Research: Planets*, *119*(5), 1046–1060. https://doi.org/10.1002/2013JE004519

Stein, T. C., Arvidson, R. E., Bommel, V., Wagstaff, K. L., & Zhou, F. (2019). MSL Analyst's Notebook: Curiosity APXS concentration data integration and Mars target encyclopedia and interface updates, 50th LPSC. Retrieved from https://www.hou.usra.edu/meetings/lpsc2019/pdf/1820.pdf